Effect of Anions on the Binding and Oxidation of Divalent Manganese and Iron in Modified Bacterial Reaction Centers

Kai Tang,[†] JoAnn C. Williams,[‡] James P. Allen,[‡] and László Kálmán[†*]

[†]Department of Physics, Concordia University, Montreal, Quebec, Canada; and [‡]Department of Chemistry and Biochemistry, Arizona State University, Tempe, Arizona

ABSTRACT   The influence of different anions on the binding and oxidation of manganous and ferrous cations was studied in four mutants of bacterial reaction centers that can bind and oxidize these metal ions. Light-minus-dark difference optical and electron paramagnetic resonance spectroscopies were applied to monitor electron transfer from bound divalent metal ions to the photo-oxidized bacteriochlorophyll dimer in the presence of five different anions. At pH 7, bicarbonate was found to be the most effective for both manganese and iron binding, with dissociation constants around 1 μM in three of the mutants. The pH dependence of the dissociation constants for manganese revealed that only bicarbonate and acetate were able to facilitate the binding and oxidation of the metal ion between pH 6 and 8 where the tight binding in their absence could not otherwise be established. The data are consistent with two molecules of bicarbonate or one molecule of acetate binding to the metal binding site. For ferrous ion, the binding and oxidation was facilitated not only by bicarbonate and acetate, but also by citrate. Electron paramagnetic resonance spectra suggest differences in the arrangement of the iron ligands in the presence of the various anions.

INTRODUCTION

Bacterial reaction centers (BRC) from purple photosynthetic bacteria are arguably among the most widely studied membrane proteins that perform electron transfer reactions. The BRCs were the first membrane proteins whose structures were revealed at atomic resolution, and this structure served for many years as a model for photosystem II (PS II) before that structure was finally determined (1–4). Comparison of these structures shows similarities between the core subunits of PSII and BRC—namely, five transmembrane alpha helices in their D1, D2 and L, M subunits, respectively—that incorporate the array of cofactors arranged in a twofold symmetry. Upon excitation by light, both the BRC and the PSII transfer an electron across the membrane from the primary electron donor to the quinones via an essentially unidirectional path involving intermediate electron acceptors along one of the branches (5,6). Upon the transfer of two electrons, the secondary quinone becomes doubly reduced and doubly protonated and is replaced by a new quinone and the cycle repeats. This quinone chemistry is a vital step in establishing a vectorial proton transfer across the photosynthetic membrane that eventually provides ATP synthase with protons.

To maintain the continuous cycle, secondary electron donors are needed to reduce the primary electron donor. For PSII and BRC, these reactions are radically different. PS II has a unique ability to utilize water as a terminal electron donor, using a tyrosine residue and a tetranuclear manganese complex as intermediate electron donors (5).

Native BRCs utilize cytochromes as secondary donors, because neither the oxidizing potential of the primary electron donor (P) nor the metal binding ability of its vicinity is sufficient to use most metal ions or tyrosine residues as secondary electron donors.

Based on the structural similarities between PSII and BRC, a series of genetically modified BRCs were designed and constructed to enable BRCs to perform reactions observable in PSII. The oxidation potential of P in BRCs was increased to a level that was suitable for both tyrosine and manganese oxidation (7–9).The availability of mutants with highly oxidizing primary electron donors opened the door for additional changes that would make the BRC capable of performing reactions not possible in the wild type. Introduction of tyrosine residues near the special pair of bacteriochlorophylls in various positions to highly oxidizing reaction centers resulted in utilization of those tyrosines as secondary electron donors (8–11). The high potential alone was sufficient to utilize Mn^{2+} as a secondary electron donor to P^+ in a diffusion-controlled, second-order reaction at pH 9 (9). Because of the lack of high-affinity binding sites in those BRCs, high (mM) concentrations of manganese were required to reduce P^+.

Four different metal binding sites were designed by introducing carboxyls ~10 Å from P at a location analogous to the site of the manganese cluster in PSII. Three of the four mutants showed high affinity for binding manganese, with dissociation constants ranging between 1 and 10 μM at around pH 9 (12). The tight binding allowed the Mn^{2+} to be an efficient secondary electron donor to P^+, with first-order rate constants for the metal oxidation exceeding the rate constants of the competing charge recombination at pH 9 by nearly fourfold (9,12). It was demonstrated that the K_D values for

manganese binding in these mutants are highly dependent on pH and tight binding could only be established above pH 8, whereas the weaker manganese binding at lower pH values needed to be stabilized by the release of two protons (13). In the presence of bicarbonate, Fe^{2+} was bound even at pH 7 with a dissociation constant of 1 μM, and rapid, first-order electron transfer was observed from the bound Fe^{2+} to P^+ (14).

Bicarbonate and other anions have been reported to play important roles in facilitating the binding of iron or manganese to proteins. Various transferrins, a family of iron transport proteins, require bicarbonate or phosphate as a synergistic anion for iron binding (15,16). An involvement of bicarbonate in the assembly of the tetranuclear manganese complex of PSII has been proposed (17,18). A recent work, however, showed that bicarbonate is not present in the assembled oxygen evolving complex (OEC) (19). Hence, the role of the bicarbonate appears to be limited to the assembly of the OEC. Based on the involvement of anions in metal binding in these proteins, the influence of different anions on properties of the four mutants was investigated. The binding and the electron transfer between the divalent metal ions and P^+ was characterized using light-minus-dark optical and electron paramagnetic resonance (EPR) spectroscopies in the presence of different anions. The binding of metal is discussed in comparison with other metal binding proteins that utilize synergistic anions.

MATERIALS AND METHODS

Construction and growth of the mutants

The design, construction, and growth of the mutants were described earlier (7,12,20,21). The highly oxidizing potential of P has been achieved by introducing three hydrogen bonds with His substitutions into the M197, L131, and M160 positions, with modifications as described in the Supporting Material.

The mutants were grown semiaerobically in the dark for 3–4 days at 30°C. The isolation of the BRCs was performed as described earlier (22), with the following modifications: The ion exchange chromatography was carried out in 0.05% Triton X-100 instead of in 0.1% lauryl dimethylamine oxide. The BRCs were dialyzed extensively for 24–48 h using 0.05% Triton X-100, 15 mM Tris-HCl (pH 8) or Hepes (pH 7) to remove EDTA, a potent chelator for metals. Measurements were carried out after addition of 100 μM terbutryne to block the electron transfer between the quinones. Ferrous sulfate and manganous chloride stock solutions were prepared before the measurements using degassed distilled water. Autooxidation of the metals was prevented by saturating the gas phase above the samples and stock solutions with nitrogen and by sealing the vessels and cuvettes with parafilm. For the pH-dependent manganese binding, the following buffers were used to adjust the pH: Mes (2-(N-morpholino)ethanesulfonic acid), pH 5.6–6.7; Hepes, pH 7.0–8.0; Tris (Tris(hydroxymethyl)aminomethane), pH 7.6–8.8; and Ches (2-(N-cyclohexylamino)ethane sulfonic acid), pH 8.6–9.4.

Optical and EPR spectroscopy

Varian (Mulgrave, Victoria, Australia) Cary 5 and 5000 spectrophotometers were used to measure the light-induced absorption changes generated by continuous illumination. The light excitation was achieved by using Oriel tungsten lamps with bandpass interference filters with maximum transmittance at 860 nm. The illumination lasted only while the spectra were recorded

in the 700–1000 nm spectral range with ~900 nm/min scanning rate. Laser-flash-induced absorption changes were recorded with either a single beam spectrophotometer of local design (23) or a miniaturized laser flash photolysis (LFP-112) system with the NIR sensitive photomultiplier (Luzchem Research, Ottawa, Ontario, Canada). The BRCs were excited with laser pulses of 5-ns duration generated by Nd:YAG lasers (Continuum, Santa Clara, CA), and the kinetic traces were analyzed by decomposition of the recorded traces into exponentials using Marquardt nonlinear least squares method.

Light-minus-dark EPR difference spectra were recorded at 120 K with a Bruker (Silberstreifen, Germany) E580 X-band spectrometer equipped with an Oxford (Oxford Instruments, Oxfordshire, UK) 900 EPL cryostat. The samples for the EPR measurement were prepared as described earlier to avoid the presence of excess free metal ions (14). Spectra were measured first in samples frozen in the dark, and then the light-induced species were generated by rapidly freezing the samples promptly after the illumination was turned off. The analysis of the data was adapted in part from Gerencsér and Maróti (24) and is described in detail in the Supporting Material.

RESULTS

Spectral changes caused by the combined presence of manganese and bicarbonate

In the absence of any metal ion, the light-minus-dark optical spectra of the M1 mutant in the near-infrared spectral range showed distinct features characteristic of both P^+ and Q_A^- when terbutryne was present at pH values 7.0 and 9.0 (Fig. 1, a and b, trace 1). These features include the bleaching of the Q_y band of the dimer centered around 865 nm, a hypsochromic shift of the band assigned to the bacteriochlorophyll monomers around 800 nm due to the positive charge on the nearby P^+, and a bathochromic shift on the absorption band of the bacteriopheophytins around 760 nm associated with the negative charge on the neighboring Q_A^-. These features were independent of pH and very similar to those reported for wild-type and the M2-mutant BRCs (8,12). Upon addition of manganous ions at a concentration of 100 μM, the spectra underwent significant changes in a very pronounced pH-dependent manner. While at pH 7.0, essentially no change was observed because of the addition of the metal (Fig. 1 a, trace 2); the spectral features characteristic of P^+ disappeared at pH 9.0 (Fig. 1 b, trace 2), resulting in a spectrum characteristic of Q_A^- (25). These spectral signatures are consistent with the presence of a bound secondary electron donor to P^+ at pH 9.0 but not at pH 7.0 (13). Addition of 15 mM sodium bicarbonate to the same assay solutions containing the BRCs and the manganese did not cause any further changes at pH 9.0 (Fig. 1 b, trace 3), but it eliminated the spectral signatures of P^+ at pH 7.0 (Fig. 1 a, trace 3). This observation suggests that the bicarbonate is required for the binding and oxidation of the manganese at pH 7.0 (13). Addition of only bicarbonate but not the manganous ion had no effect on the $P^+Q_A^-$ charge pair, and the recorded spectra were practically indistinguishable from those labeled as trace 1 in Fig. 1, a and b, at either pH 7.0 or 9.0 (data not shown). In all cases, within 15 min after the illumination was stopped, the absorption changes recovered, indicating that the light-induced changes were fully reversible.
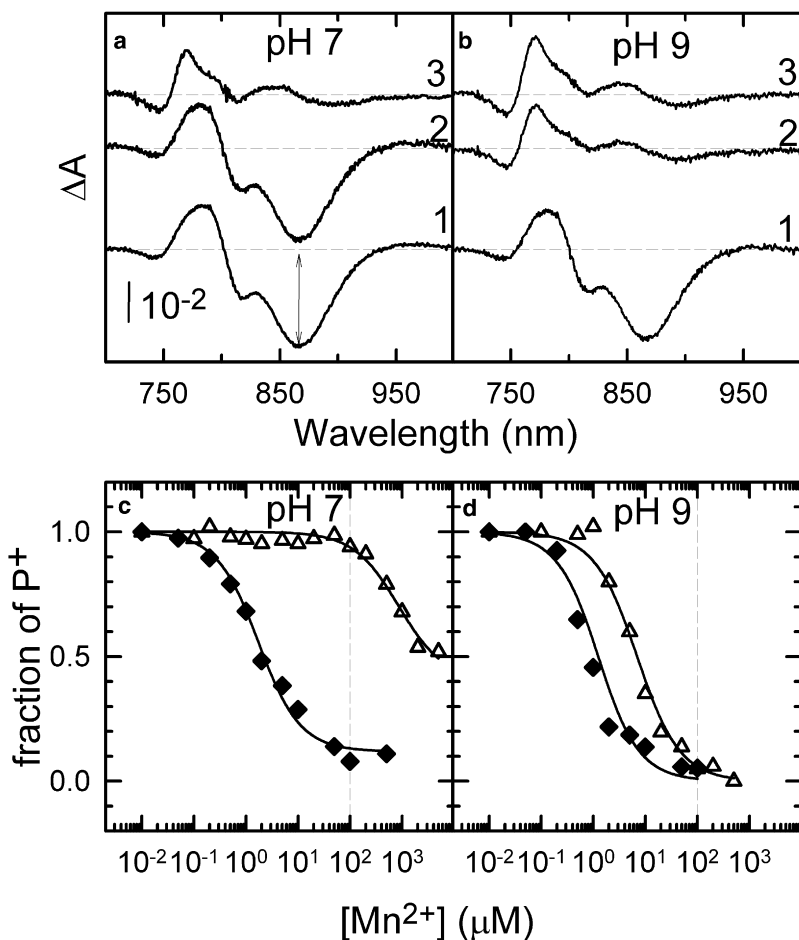
FIGURE 1 (*a* and *b*) Light-minus-dark difference optical spectra of the M1 mutant at pH 7 and pH 9 in the absence of either manganese or bicarbonate ions (*trace 1*), in the presence of 100 μM manganese (*trace 2*), and in the presence of both 100 μM manganese and 15 mM bicarbonate ions (*trace 3*). (*c* and *d*) Fraction of P^+ as a function of the added Mn^{2+} concentration measured in the M1 mutant at pH 7 and pH 9 in the absence (*open triangles*) and in the presence of 15 mM bicarbonate (*solid diamonds*). The data points were taken from the light-minus-dark difference spectra recorded at various manganese concentrations as the absorbance changes at 865 nm as indicated, with the double-headed vertical arrow on panel *a*. The solid lines are the best fits to the data points using Eq. S2 with the following dissociation constants: 853 μM and 1.5 μM at pH 7, and 6.2 μM and 1.0 μM at pH 9 in the absence and in the presence of 15 mM bicarbonate, respectively. The vertical dashed lines in panels *c* and *d* drawn at 100 μM manganese concentration indicate the condition at which the spectra on panels *a* and *b* were recorded. Conditions: 1.5 μM BRC in 0.03 Triton X-100, 100 μM terbutryne, 15 mM Hepes (pH 7), or Ches (pH 9).

The manganese concentration was increased systematically from 0 to 1 mM, and the light-minus-dark difference optical spectra were recorded in the presence and in the absence of bicarbonate both at pH 7.0 and 9.0. Using the method determined earlier for these mutants, the fraction of P^+ was plotted as a function of the applied manganese concentration (Fig. 1, *c* and *d*) to determine the dissociation constants (K_D) of manganese binding (Eq. S2) (12). In the presence of 15 mM bicarbonate, the K_D was found to decrease from 830 μM to 1.5 μM at pH 7, and from 6.2 μM to 1.0 μM at pH 9 in the M1 mutant, compared to results with the bicarbonate-free systems.

pH dependence of manganese binding and oxidation in the presence of various anions

In addition to bicarbonate, the effect of other anions, acetate, borate, phosphate, and citrate on the binding and oxidation of manganese to the M1 mutant was investigated. Only bicarbonate lowered the K_D of manganese binding significantly, acetate and citrate were less effective, and malate and phosphate had little effect (Table S1). The pH dependence of the dissociation constant for manganese binding in the four mutants was studied in detail in the presence of bicarbonate

and acetate as described in Fig. 1. The values of K_D for manganese binding were strongly dependent on the pH in the presence of bicarbonate and acetate (Fig. 2). In the absence of anions, the dissociation constants of three mutants, M1, M2, and M4, exhibited a strong pH dependence with high values at pH 7.0 and a steep, two orders of magnitude per pH unit decrease between pH 7.0 and ~8.5 (13). Between pH 8.5 and 9.0, K_D was independent of pH, and the tightest binding was observed with K_D varying between 1 and 10 μM depending on the mutant. The fourth mutant, M3, exhibited large values of K_D for all pH values, even in the presence of the anions. In the presence of 15 mM bicarbonate between pH 6.5 and 8.0, the dissociation constants were lower for the M1, M2, and M4 mutants than those for the cases without any added anions. For these three mutants, K_D was found to be independent of pH between pH 6.5 and 9.0, with values ranging between 1 and 5 μM, suggesting very strong binding in this wide pH range. Below pH 6.0 the values of K_D increased steeply with decreasing pH. These values of K_D were significantly lower than were those measured without bicarbonate; for example, at pH 7.0, K_D decreased by close to three orders of magnitude.

The pH dependence was modeled by assuming the involvement of two amino-acid side chains that change their
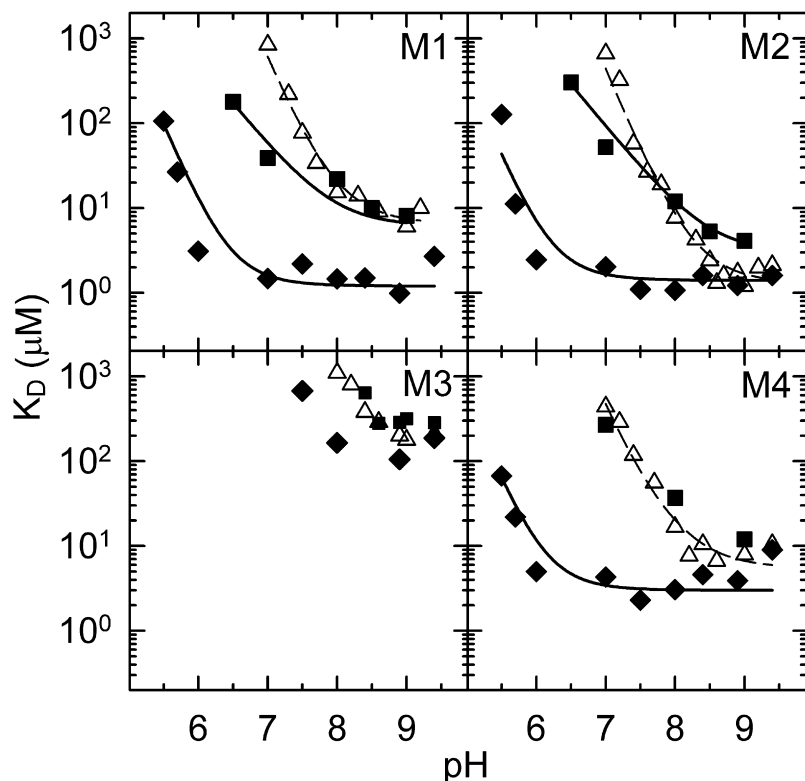
FIGURE 2 pH-dependence of the dissociation constant (K_D) for manganese binding in the M1, M2, M3, and M4 mutants in the absence of any added anion (*open triangles*), in the presence of 15 mM bicarbonate (*solid diamonds*), and in the presence of 100 mM acetate (*solid squares*). The solid lines are the best fits using Eq. S3, assuming two interacting residues with indistinguishable pK values for bicarbonate and (Eq. S4) assuming one residue for acetate. The open symbols and dashed lines representing the data without any added anion are taken from Kálmán and colleagues (13) for comparison. The following values were obtained for the dissociation constants ($K_D{}^0$) for the strongest binding in the presence of bicarbonate: 1.2, 1.4, and 3.0 μM for M1, M2, and M4 mutants, respectively. In the same order the pK(c) values are: 6.43, 6.20, and 6.11. The $K_D{}^0$ and pK(c) values in the presence of acetate are: 6.2 μM and 7.9, and 3.0 μM and 8.5 in the M1 and M2 mutants, respectively. Conditions as in Fig. 1, except that 15 mM Mes, Hepes, Tris or Ches were used, depending on pH.

protonation state to facilitate binding of the divalent manganese (Eq. S3). The fit yielded values for $K_D{}^0$ and pK(c) of 1.2 μM and 6.42 for the M1 mutant, 1.4 μM and 6.2 for the M2 mutant, and 3 μM and 6.11 for the M4 mutant, respectively. In the presence of bicarbonate the pK(c) values shifted ~2 pH units toward lower pH values compared to those with the anion-free cases reported earlier (13). Above pH 9.0, a small increase in the apparent K_D values was observed in all mutants, and it was more pronounced in the presence than in the absence of bicarbonate. The most plausible explanation for this effect is that the bicarbonate/carbonate equilibrium has a pK value of ~10.0 in aqueous solutions, and, as the pH increases, the carbonate can react with manganese to form an insoluble manganous-carbonate. This behavior was more visible in the M1 and M4 mutants, where, in the presence of bicarbonate, $K_D{}^0$ was lower than it was in the absence of it at pH 9.0, whereas, in the M2 mutant, $K_D{}^0$ was approximately the same with and without bicarbonate (1.4 and 1.2 μM, respectively) at this pH. This pH dependence suggests that the bicarbonate most likely participates in metal binding even at pH values above 8.0. In addition, the manganese can also form manganous-hydroxide at high pH values, which is also insoluble. These events can decrease the activity of the manganese and/or the bicarbonate and set the upper pH limit for our measurements between pH 9.0 and 9.4.

The effect of acetate on the pH dependence of K_D is significantly different from that of bicarbonate (Fig. 2). Below pH 8 in the M1 and M2 mutants, the presence of 100 mM acetate clearly lowered the K_D for manganese binding, but acetate seemed to have a minor effect on K_D above pH 8.0 in the M1 mutant and it appeared to have no effect at all at any pH in the M3 and M4 mutants. For example, at pH 7.0, the dissociation constant measured for the M1 mutant had a value of 39 μM in the presence of acetate compared to the value of 830 μM in its absence. The K_D decreased only slightly from 22 μM to 13 μM because of the presence of acetate at pH 8.0. In the M2 mutant above pH 8.0, the presence of acetate slightly decreased the binding affinity of the manganese compared to the affinity in the anion-free case. The pH dependence of K_D in the M1 and M2 mutants is described better with Eq. S4, which assumes the involvement of only one protonatable residue in the electrostatic stabilization of the metal binding, than with Eq. S3, which assumes the involvement of two protonatable residues.

Dependence of K_D on the concentration of the anions

The dependence of the dissociation constant for manganese binding on the added bicarbonate or acetate concentration was measured for the M1 mutant at pH 7.0 (Fig. 3). For quantitative analysis, the negative logarithm values of the molar anion concentrations (pA) are used instead of the concentrations themselves. Without any added anion, the manganese binding is very weak at pH 7.0, with a K_D value of 830 μM. As the concentration of the anions was increased, K_D began to decrease at 100 μM and 1 mM concentrations of
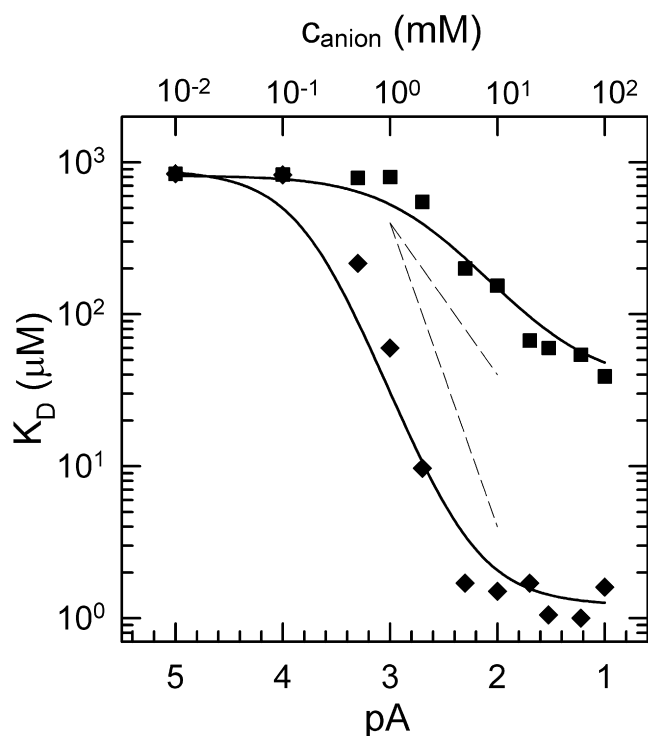
FIGURE 3 Dependence of the dissociation constant (K_D) of manganese binding on the negative logarithm of added pA for bicarbonate (*diamonds*) and acetate (*squares*) at pH 7. The K_D values were determined as shown in Fig. 1 in the presence of bicarbonate and acetate at various concentrations. The data points were fitted with Eq. S5 and Eq. S6, assuming two molecules of bicarbonate and one molecule of acetate facilitating the metal binding, respectively. The dashed lines indicate −2 decades/pA and −1 decade/pA slopes. The fit resulted in $K_D{}^0$ values of 1.2 μM and 35 μM for bicarbonate and acetate, respectively. The pAK and pAK' values are 5 mM and 180 μM for bicarbonate and 40 mM and 1.7 mM for acetate, respectively. Conditions as in Fig. 1.

bicarbonate and acetate, respectively. The values for K_D with increasing bicarbonate concentration decreased by about two orders of magnitude/pA with decreasing pA, whereas, in the presence of acetate, the rate of decrease was closer to one order of magnitude/pA. At high anion concentrations, K_D values leveled off to values of ~1 μM and ~ 40 μM for bicarbonate and acetate, respectively. The pA dependences of K_D were well described, assuming the presence of two bicarbonate ions (Eq. S5) or one acetate ion (Eq. S6) facilitating the binding and oxidation of manganese. The resulting fits yielded values of 1.2 and 35 μM for $K_D{}^0$ for bicarbonate and acetate, respectively. The pAK' and pAK values were 180 μM and 5 mM for bicarbonate and 1.7 mM and 40 mM for acetate.

Rate of manganese oxidation

The kinetics of the P^+ recovery after a laser-flash excitation were studied in the M1 and M2 mutants at pH 7.0 and 9.0 in the presence and absence of acetate and bicarbonate (Fig. 4). Terbutryne was included to block the electron transfer

between the primary and secondary quinones. A manganese concentration of 100 μM was selected to probe the kinetics of electron donation to P^+ as the dissociation constants were below 50 μM between pH 7.0 and 9.0 in both mutants. In the absence of manganese, the kinetic traces could be well characterized with single exponential functions with rate constants (k_{AP}) between 23 and 27 s^{-1} depending on the mutant and pH. This kinetic component was assigned to $P^+Q_A{}^- \rightarrow PQ_A$ charge recombination. In the presence of manganous ions at a concentration of 100 μM, the recovery of P^+ became faster and biphasic if both of the following two conditions were met: i), the manganese was bound to the designed binding site in the BRC, and ii), the electron transfer from the bound metal ion to P^+ was faster than the $P^+Q_A{}^- \rightarrow PQ_A$ charge recombination by a factor of at least two. For example, in the absence of bicarbonate, the kinetics of P^+ recovery did not change on addition of 100 μM manganese at pH 7.0 (Fig. 4 *a*), because the metal was only weakly associated with the BRC ($K_D \approx$ 1 mM) at this pH, but it became significantly faster at pH 9.0 because of the presence of a second kinetic component with a rate constant of ~90 s^{-1} and 87% contribution to the total signal (Fig. 4 *b*). This faster kinetic component was attributed to the Mn^{2+}-$P^+Q_A{}^- \rightarrow$ Mn^{3+}-$PQ_A{}^-$ electron transfer reaction from the bound manganese, becuase the rate constant was found to be independent of the metal concentration (12). Any contribution to the kinetic traces from a nonbound manganese could be ruled out based on an earlier study, in which we showed that the electron transfer in the diffusion controlled process at 100 μM manganese concentration is slower than the $P^+Q_A{}^- \rightarrow PQ_A$ charge recombination of the M1 and M2 mutants (9). In the presence of bicarbonate, the recovery of P^+ accelerated even at pH 7.0 on addition of 100 μM manganese (Fig. 4 *c*). The faster kinetic component, which was assigned to the manganese oxidation, had a rate constant (k_{MnP}) of 48 s^{-1} and it represented 62% of the total signal. As the pH was raised from 7.0 to 9.0 in the presence of bicarbonate, the rate constant of the fast component increased by ~2-fold (Fig. 4 *d*), but this value was only ~10% higher than the rate constant for manganese oxidation at pH 9.0 without the bicarbonate.

The rate constants increased as the pH increased for both the M1 and M2 mutants (Fig. 5). In the absence of the anions, the manganese oxidation could be measured only above pH 7.8 because of limited manganese binding. The k_{MnP} values increased by 23–28% as the pH was raised from pH 8.0 to 9.0 and were generally ~30% larger in the M2 mutant compared to values in the M1 mutant. As the pH was raised from 7.0 to 9.0, the rate constant of manganese oxidation increased by a factor of ~2, with a nearly linear pH dependence in both mutants. In the presence of acetate, k_{MnP} values could be determined only above pH 8.0 and were generally lower than those in the presence of bicarbonate. Interestingly, whereas, in the M1 mutant the k_{MnP} values for acetate above pH 8.0 were similar to those
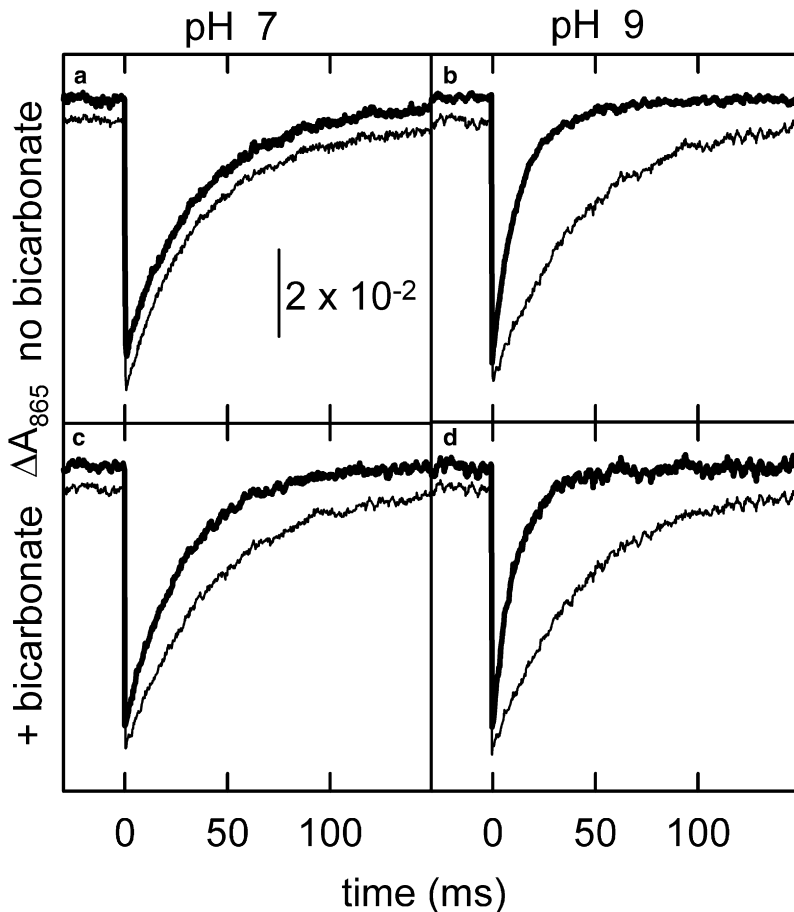
FIGURE 4   Kinetic traces of P^+ reduction in the presence of 100 μM terbutryne monitored at 865 nm in the M2 mutant after a saturating laser flash excitation at pH 7 (*a* and *c*) and at pH 9 (*b* and *d*) in the absence (*a* and *b*) and in the presence (*c* and *d*) of 15 mM bicarbonate, respectively. The kinetics were recorded after a saturating laser flash. The traces with thin lines were recorded without any added manganese and could be fitted with single exponentials representing the kinetics of $P^+Q_A^- \rightarrow PQ_A$ charge recombination with rate constants of 23–24 s^{-1}. The traces with thick lines, which are vertically shifted for better comparison, were recorded in the presence of 100 μM Mn^{2+} ions, and, except in panel *a*, the P^+ decay could be resolved into two kinetic components. The faster component was assigned to the P^+ reduction by Mn^{2+} and the slower to the $P^+Q_A^- \rightarrow PQ_A$ charge recombination. The kinetic analysis resulted in the following rate constants and the relative amplitudes: 24 s^{-1} (100%) for panel *a*; 23 s^{-1} (13%) and 91 s^{-1} (87%) for panel *b*; 24 s^{-1} (38%) and 48 s^{-1} (62%) for panel *c*; and 23 s^{-1} (8%) and 100 s^{-1} (92%) for panel *d*. Conditions as in Fig. 1.

without any added anion, in the M2 mutant the rate constants were higher without any anion than those with added acetate. This observation agrees with the elevated K_D value in the M2 mutant at high pH in the presence of acetate.
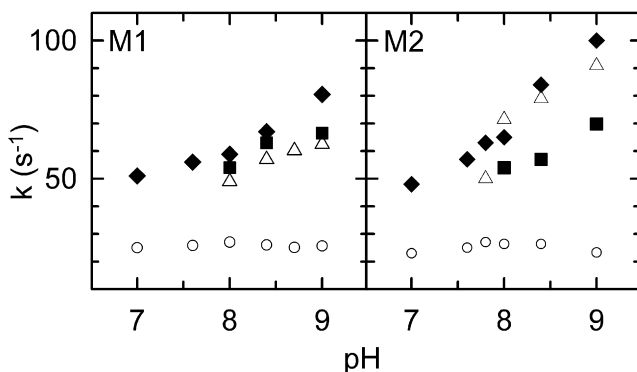

FIGURE 5   pH dependence of first-order rate constants of manganese oxidation in the M1 (*left panel*) and M2 (*right panel*) mutants. The rate constants were determined by the exponential decomposition of the kinetics recorded in the presence of 100 μM Mn^{2+} and in the absence of any anion (*open triangles*), in the presence of 15 mM bicarbonate (*solid diamonds*), and in the presence of 100 mM acetate (*solid squares*). The rate constants for $P^+Q_A^- \rightarrow PQ_A$ (*open circles*) are also shown. Conditions as in Fig. 2.

Iron oxidation in the presence of anions

It has been shown earlier that ferrous ions can be bound to the M1 and M2 mutants and can serve as efficient electron donors to P^+ in the presence of bicarbonate at pH 7.0 (14). One advantage is that the bound oxidized iron, unlike bound manganese, is expected to have a distinctive EPR signal. In addition, the driving force for electron transfer from the ferrous ion should be larger than that for manganese because of the significantly lower oxidation/reduction midpoint potential of the Fe^{2+}/Fe^{3+} couple compared to that of the Mn^{2+}/Mn^{3+} couple. A disadvantage of using iron is that pH- dependent studies cannot be performed, because of the limited solubility and possibly the increased rate of autooxidation of the Fe^{2+} at pH values other than 7.0.

Light-minus-dark X-band EPR difference spectra were measured for the M1 mutant with added Fe^{2+} in the presence of bicarbonate, malate, acetate, phosphate, and citrate, and without any anions at pH 7.0 (Fig. S1). The line shape of the EPR signals near *g* values of 4.3 are characteristic of that of hexacoordinated high-spin ferric iron, and it showed distortions from the isotropic line expected from a completely rhombic Fe^{3+}. Line broadenings and unresolved splittings suggest that the signal arises from a bound ferric ion and indicate that the coordination geometry of the iron in the

M1 mutant is different in the presence of various anions. The peak-to-trough line widths ranged between 24 and 51 Gauss (Table S1). The spectra collected in the dark before the illumination are also shown for comparison, and their amplitudes were found to be between 6 and 17% of the total signals.

The rate constants for iron oxidation in the presence of these anions showed a range of values between 96 and 275 s^{-1} (Table S1). The observed rate constants were independent of the iron concentration only for bicarbonate, acetate, and citrate. A slight increase in the rate constants was observed as the iron concentration was increased in the presence of phosphate, malate, and without any anion. Based on the very similar dissociation constants ($K_D \approx 30\ \mu$M) and rate constants for iron oxidation ($k_{FeP} \approx 100\ s^{-1}$), as well as on the very similar ferric EPR signals for phosphate, malate, and without any anion, we concluded that malate and phosphate most likely do not participate in the binding at all.

DISCUSSION

In this work, the highly oxidizing reaction centers with designed metal binding sites have been shown to bind manganese tightly and oxidize the metal in the entire pH range of 7 to 9 only if bicarbonate was present (Fig. 1). The binding affinity of the manganese was found to be independent of pH between pH ~6.0 and 9.0 in the presence of bicarbonate in three of the four mutants (M1, M2, and M4), with dissociation constants between 1 and 3 μM (Fig. 2). Below pH 6.0, the value of K_D increased steeply and the entire pH dependence was described by the participation of two titrating residues with very close pK values, representing the pK of the entire cluster (pK(c)). For all three mutants, the fit yielded very similar pK(c) values ranging between 6.1 and 6.5 (Fig. 2). These pK(c) values were ~2 pH units lower than those reported for the absence of any anions, indicating that the presence of the bicarbonate extends the ability of these mutants to establish tight binding with manganese over three pH units (13). The obtained pK(c) values were in good agreement with the reported pK values for the carbonic acid/bicarbonate system in aqueous disperse systems containing detergent micelles, suggesting that the bicarbonate/carbonic acid equilibrium governs the binding of the metals (26). Of the other tested anions, only acetate altered the pH dependence of K_D. The pH dependence of K_D could be described by assuming that only one titrating group participates in manganese binding for the M1 and M2 mutants, and, in the M3 and M4 mutants, the effect of acetate on the binding was not significant.

The dependence of K_D in the presence of acetate and bicarbonate on pH (Fig. 2) and on the concentration of the anions (Fig. 3) strongly suggests that either two bicarbonates or one acetate are associated with the manganese upon binding in the presence of these anions. For two bound bicar-

bonates, the charge on the divalent metal is compensated by the negative charges on the two bicarbonates. The charge compensation eliminates the need for proton release from amino-acid side chains and results in K_D being independent of pH. Below pH 6.0, the bicarbonate becomes protonated and forms carbonic acid, which in turn dissociates to carbon dioxide and water. Thus, below pH 6.0, the binding becomes strongly pH dependent, with the necessity of the proton release. In the presence of acetate, however, it was found that only one acetate is associated with the binding of the manganese (Fig. 3), resulting in a pH dependence of K_D that could be described with the release of one proton from the amino-acid side chains below pH 8.0. The binding of one acetate per manganese, compared to two bicarbonates per manganese, may be due to the larger size of acetate compared to that of bicarbonate, as discussed below.

It has been reported that the manganese can form $Mn^{II}(HCO_3)^+$ and $Mn^{II}(HCO_3)_2$ complexes, depending on the bicarbonate concentration, by exchanging one or two coordinating water molecules with bicarbonate in the hexa-aquo complex (27,28). These associations are weak and require relatively high (mM) bicarbonate concentrations to generate them, with reported binding energies of 26 and 44 kJ/mol for the $Mn^{II}(HCO_3)^+$ and $Mn^{II}(HCO_3)_2$ complexes, respectively (27). The electrostatic stabilization by the coordination with bicarbonate also lowers the oxidation/reduction midpoint potential of the Mn^{2+}/Mn^{3+} couple in aqueous solutions from 1.2 V in the hexa-aquo complex to 0.92 and 0.63 V if one or two bicarbonates were bound to the manganese, respectively (27–29). Acetate is known to inhibit oxygen evolution in PSII, possibly by replacing the Cl$^-$ cofactor. Typically, 400–500 mM acetate is used to inhibit PSII (30,31).

Binding to the protein should alter the midpoint potential of the manganese and modify the driving force, with a pH dependence analogous to the pH dependence of K_D. The reported values of the rate constants for manganese and iron oxidation with and without the anions are consistent with electron transfer occurring within 15 Å, even if the reorganization energies are relatively high (32). Based on the extent of P$^+$ reduction in BRCs without a metal binding site, the pH dependence of the midpoint potential for the Mn^{2+}/Mn^{3+} couple in the presence of bicarbonate can be characterized with a −63 mV/pH slope (9). This midpoint potential likely represents the potential of the metal in solution, because the association between the metal and the BRC without the binding site was weak ($K_D \approx 100\ \mu$M) and the reactions were classified as second-order processes. The rate constants for iron oxidation in the presence of bicarbonate in the M1 mutant at pH 7 are more than fivefold higher than those for manganese at the same pH (Table S1; Fig. 5). The oxidation/reduction midpoint potential of the Fe^{2+}/Fe^{3+} couple at pH 7.0 is reported as ~0.2 V (33). If one assumes the reorganization energy to be the same as that for manganese, then the driving force for iron oxidation should be more than

500 meV higher than that for manganese oxidation. Experiments are underway to determine the midpoint potential of the bound manganese.

Structural requirements accommodating the anions

X-ray crystallographic analysis identified that in the M2 mutant in the absence of anions the ligands that coordinate the bound manganese without added anions are Glu-M168, Glu-M173, His-M193, Asp-M288 and one water molecule (12). The Tyr-M164 is also in the close vicinity of the metal. A structural model has been developed for the most probable positions of the two bicarbonates proposed to bind at the metal binding site (Fig. 6). The bicarbonate molecules were positioned in the structure such that the repulsion between the bicarbonates and the carboxylic oxygen atoms on Glu-M168, Asp-M288 and Glu-M173 was minimized. The different line shapes in the EPR spectra of the M1 mutant, arising from bound ferric ion, suggest slight differences in the geometry of the metal binding site in the presence of different anions (Fig. S1). Although we have available structural information only for the M2 mutant, the role of Asp-M288 is most probably taken by Glu-M192 in the M1 mutant.

Anions, specifically (bi)carbonate, have been proposed as facilitators for metal binding in different enzymes, such as PSII and various transferrins (16,34,35). In PSII the bicarbonate was assigned not only as a metal stabilizing ligand during the photoassembly of the OEC, but also as an evolutionarily important component of the development of PSII from BRC-like ancestors (29,36). However, only one of the available 3D structures models the bicarbonate in the OEC of PSII (37). Functional studies have yielded contradictory conclusions regarding the role of the bicarbonate in the OEC (19,28). Comparison of the metal binding pockets shows Glu-M173, His-M193 and Tyr-M164 in the metal-binding BRC are located at similar positions as Asp-D1-170, His-D1-190 and Tyr-D1-161 in PSII (Fig. 6). The 3D structures of various transferrins show the placement of (bi)carbonate in the iron binding site (38–40). The binding site of the iron in the C-lobe of ovotransferrin contains a pair of residues, Tyr-191 and His-250, whose relative positions are similar to those of the Tyr-M164 and His-M193 pair

of BRC and the Tyr-D1-161 and His-D1-190 pair of PSII. The other four ligands of the iron are Tyr-92 and Asp-59, and a (bi)carbonate as a bidentate ligand. It is noticeable that, for tight binding, all six coordination sites should be occupied by an approximate octahedral geometry. In the manganese binding pocket of the BRC, four residues were identified as the most probable ligands based on the 3D structure and geometry optimization (12). Two sites were available beneath and above the bound metal for the anions. In the case of the bulkier acetate, it seems that there is not enough space to accommodate the second molecule beneath the manganese. The binding of the (bi)carbonate molecules was proposed to be facilitated by Arg-121 in the ovotransferrin and Arg-357 in the CP-43 subunit in the OEC (38,37). It is unclear, however, what residue might coordinate the bicarbonate in the BRC, because there was no arginine near the binding pocket. Earlier studies for transferrins suggested that the bicarbonate ion could be hydrogen-bonded to one of the tyrosine residues in the pocket (16). This option is possible, because the Tyr-M164 is below the bound metal but is too far to serve as a ligand to the metal (Fig. 6 *a*). Hydrogen bonding to the Tyr-M164 could anchor the bicarbonate in the pocket.

Role of the synergistic anion

The anions enhance the binding of divalent metal ions at pH values lower than 9.0. The efficiency of manganese binding is strongly influenced by the pK values of the ligands in the binding cluster at a given pH; the binding is expected to be weak if many of the coordinating residues are protonated. The pK of the cluster without added anions was reported to be between 7.9 and 8.3 in the M1, M2, and M4 mutants, and, because of manganese binding, these pK values were shifted by -1 and -1.5 pH units in the M4 and the M2 mutants, respectively (13). The exact mechanism by which the anions facilitate the low pH binding is not known. Based on electrostatic considerations, bicarbonate and acetate ions are negatively charged and, hence, unable to shift the pK values of the residues in the cluster toward lower pH values. It was reported, however, that addition of 24 mM NaHCO$_3$, a very similar concentration to that used in this study, to an unbuffered aqueous solution raised the pH of the solution
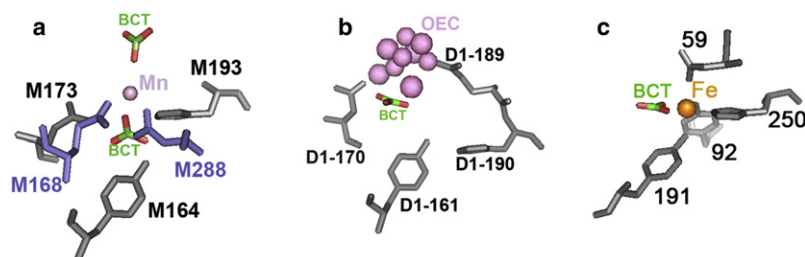

FIGURE 6 Structures of the metal binding sites in (*a*) modified BRC, (*b*) PSII, and (*c*) in the C-lobe of ovotransferrin showing the key residues. The Mn in the BRC and the OEC in PSII are shown in pink, the iron in the ovotransferrin is orange, and the carbon and the oxygen atoms in the bicarbonate (*BCT*) are colored green and red, respectively. The mononuclear manganese in BRC in the M2 mutant is coordinated by His-M193, Glu-M173 and two genetically modified residues shown in blue: Glu-M168 and Asp-M288. The OEC is coordinated by several residues from the D1 subunit and from CP43. The residues from CP43 are not shown for simplicity. The corresponding residues of Glu-M173 His-M193 and Tyr-M164 of BRC are the Asp-D1-170 His-D1-190 and Tyr-D1-161. The mononuclear ferric ion in ovotransferrin is coordinated by Asp-59, Tyr-92, Tyr-191, His-250, and a BCT as a bidentate ligand. Coordinates for the M2 mutant with the proposed bicarbonates, PSII, and ovotransferrin are from Protein Data Bank entry codes 1Z9J, 1S5L, and 1OVT, respectively (12,37,38).

from 6.5 to 8.3 (27). The bicarbonate ions may increase the surface pH in a similar manner and facilitate the deprotonation of the residues in the binding pocket by altering the local pH.

The bound anions probably alter the geometry of the binding pocket, as suggested by the differences in the EPR spectra of bound iron in the presence of different anions (Fig. S1). A slight opening of the binding pocket should increase the dielectric constant and decrease the electrostatic interactions between the side chains in the binding pocket, which can result in a lower pK of the residues in the cluster. Without added anion, the hexa aquo complex of the metal ion has two positive charges, and the poor binding to the BRC at low pH is probably due to repulsive electrostatic interactions. The only residue in the pocket that can be positively charged at low pH is M193 His. The pK value of M193 His was reported to be 7.0, based on this residue serving as a proton acceptor after oxidation of M164 Tyr in the Y_M mutant (8). The addition of two carboxylic side chains near M193 His in the M1 and M2 mutants is expected to elevate the pK of M193 His and, hence, favor the positively charged state of M193 His at pH 7.0. Bound bicarbonate may serve to neutralize the positive charge on M193 His and to provide a more favorable electrostatic environment for metal binding. Likewise, bicarbonate may facilitate the binding of the metal ions in PSII and ovotransferrin. The ultimate advantage of the presence of the anions in the metal binding pocket is to extend the ability of the metal binding toward physiologically relevant pH values.

SUPPORTING MATERIAL

Equations, a figure, and a table are available at http://www.biophysj.org/biophysj/supplemental/S0006-3495(09)00499-8.

REFERENCES

1. Deisenhofer, J., O. Epp, K. Miki, R. Huber, and H. Michel. 1985. Structure of the protein subunits in the photosynthetic reaction centre of *Rhodopseudomonas viridis* at 3Å resolution. *Nature*. 318:618–624.

2. Allen, J. P., G. Feher, T. O. Yates, H. Komiya, and D. C. Rees. 1987. Structure of the reaction center from *Rhodobacter sphaeroides* R-26: the cofactors. *Proc. Natl. Acad. Sci. USA*. 84:5730–5734.

3. Allen, J. P., G. Feher, T. O. Yeates, H. Komiya, and D. C. Rees. 1987. Structure of the reaction center from *Rhodobacter sphaeroides* R-26: the protein subunits. *Proc. Natl. Acad. Sci. USA*. 84:6162–6166.

4. Zouni, A., H. T. Witt, J. Kern, P. Fromme, N. Krauss, et al. 2001. Crystal structure of Photosystem II from *Synechococcus elongatus* at 3.8 Å resolution. *Nature*. 409:739–743.

5. Wydrzynski, T., and K. Satoh. 2005. Photosystem II: The Light-Driven Water: Plastoquinone Oxidoreductase. Springer Publishers, Dordrecht, The Netherlands.

6. Hunter, N., F. Daldal, M. Thurnauer, and J. T. Beatty. 2008. The Purple Phototrophic Bacteria. Springer-Verlag, Dordrecht, The Netherlands.

7. Lin, X., H. A. Murchinson, V. Nagarajan, W. W. Parson, J. P. Allen, et al. 1994. Specific alteration of the oxidation potential of the electron donor in reaction centers from *Rhodobacter sphaeroides*. *Proc. Natl. Acad. Sci. USA*. 91:10265–10269.

8. Kálmán, L., R. Lobrutto, J. P. Allen, and J. C. Williams. 1999. Modified reaction centers oxidize tyrosine in reactions that mirror photosystem II. *Nature*. 401:696–699.

9. Kálmán, L., R. Lobrutto, J. C. Williams, and J. P. Allen. 2003. Manganese oxidation by modified reaction centers from *Rhodobacter sphaeroides*. *Biochemistry*. 42:11016–11022.

10. Narváez, A. J., L. Kálmán, R. LoBrutto, J. P. Allen, and J. C. Williams. 2002. Influence of the protein environment on the properties of a tyrosyl radical in reaction centers from *Rhodobacter sphaeroides*. *Biochemistry*. 41:15253–15258.

11. Narváez, A. J., R. LoBrutto, J. P. Allenand, and J. C. Williams. 2004. Trapped tyrosyl radical populations in modified reaction centers from *Rhodobacter sphaeroides*. *Biochemistry*. 43:14379–14384.

12. Thielges, M., G. Uyeda, A. Cámara-Artigas, L. Kálmán, J. C. Williams, et al. 2005. Design of a redox-linked active metal site: manganese bound to bacterial reaction centers at a site resembling that of photosystem II. *Biochemistry*. 44:7389–7394.

13. Kálmán, L., M. C. Thielges, J. C. Williams, and J. P. Allen. 2005. Proton release due to manganese binding and oxidation in modified bacterial reaction centers. *Biochemistry*. 44:13266–13273.

14. Kálmán, L., R. Lobrutto, J. C. Williams, and J. P. Allen. 2006. Iron as a bound secondary electron donor in modified bacterial reaction centers. *Biochemistry*. 45:13869–13874.

15. Dhuangana, S., C. H. Taboy, D. S. Anderson, K. G. Vaughan, P. Aisen, et al. 2003. The influence of the synergistic anion on iron chelation by ferric binding protein, a bacterial transferrin. *Proc. Natl. Acad. Sci. USA*. 100:3659–3664.

16. Harris, W. R., D. Nesset-Tollefson, J. Z. Stenback, and N. Mohamed-Hani. 1990. Site selectivity of binding of inorganic anions to serum transferrin. *J. Inorg. Biochem*. 38:175–183.

17. Klimov, V. V., and S. V. Baranov. 2000. Bicarbonate requirement for the water-oxidizing complex of photosystem II. *Biochim. Biophys. Acta*. 1503:187–196.

18. Ananyev, G. M., L. Zaltsman, C. Vasko, and G. C. Dismukes. 2001. The inorganic biochemistry of photosynthetic oxygen evolution/water oxidation. *Biochim. Biophys. Acta*. 1503:52–68.

19. Ulas, G., G. Olack, and G. W. Brudvig. 2008. Evidence against bicarbonate bound in the O_2-evolving complex of photosystem II. *Biochemistry*. 47:3073–3075.

20. Diner, B. A. 2001. Amino acid residues involved in the coordination and assembly of the manganese cluster of photosystem II. Proton-coupled electron transport of the redox-active tyrosines and its relationship to water oxidation. *Biochim. Biophys. Acta*. 1503:147–163.

21. Debus, R. J. 2001. Amino acid residues that modulate the properties of tyrosine Y_Z and the manganese cluster in the water oxidizing complex of photosystem II. *Biochim. Biophys. Acta*. 1503:164–186.

22. Williams, J. C., R. G. Alden, H. A. Murchison, J. M. Peloquin, N. W. Woodbury, et al. 1992. Effects of mutations near the bacteriochlorophylls in reaction centers from *Rhodobacter sphaeroides*. *Biochemistry*. 31:11029–11037.

23. Kleinherenbrink, F. A., H. C. Chiou, R. LoBrutto, and R. E. Blankenship. 1994. Spectroscopic evidence for the presence of an iron-sulfur center similar to Fx of photosystem I in *Heliobacillus mobilis*. *Photosynth. Res*. 41:115–123.

24. Gerencsér, L., and P. Maróti. 2001. Retardation of proton transfer caused by binding of the transition metal ion to the bacterial reaction center is due to pKa shifts of key protonatable residues. *Biochemistry*. 40:1850–1860.

25. Dutton, P. L., and J. B. Jackson. 1972. Thermodynamic and kinetic characterization of electron-transfer components *in situ* in *Rhodopseudomonas spheroides* and *Rhodospirillum rubrum*. *Eur. J. Biochem*. 30:495–510.

26. Kálmán, L., T. Gajda, P. Sebban, and P. Maróti. 1997. pH-metric study of reaction centers from photosynthetic bacteria in micellular solutions: protonatable groups equilibrate with the aqueous bulk phase. *Biochemistry*. 36:4489–4496.

27. Kozlov, Y. N. A. A. K., and V. V. Klimov. 1997. Changes in the redox potential and catalase activity of Mn^{2+} ions during formation of Mn-bicarbonate complexes. *Membr. Cell Biol.* 11:115–120.

28. Baranov, S. V., A. M. Tyryshkin, D. Katz, G. C. Dismukes, G. M. Ananyev, et al. 2004. Bicarbonate in a native cofactor for assembly of the manganese cluster of the photosynthetic water oxidizing complex. Kinetics of reconstitution of O_2 evolution by photoactivation. *Biochemistry*. 43:2070–2079.

29. Dismukes, G. C., V. V. Klimov, S. V. Baranov, Y. N. Kozlov, J. DasGupta, et al. 2001. The origin of atmospheric oxygen on earth: the innovation of oxygenic photosynthesis. *Proc. Natl. Acad. Sci. USA*. 98:2170–2175.

30. Szalai, V. A., and G. W. Brudvig. 1996. Formation and decay of the S3 EPR signal species in acetate-inhibited photosystem II. *Biochemistry*. 35:1946–1953.

31. MacLachlan, D. J., and J. H. A. Nugent. 1993. Investigation of the S3 electron-paramagnetic-resonance signal from the oxygen-evolving complex of photosystem II: effect of the inhibition of oxygen evolution by acetate. *Biochemistry*. 32:9772–9780.

32. Page, C. C., C. C. Moser, X. Chen, and P. L. Dutton. 1999. Natural engineering principles of electron tunnelling in biological oxidation-reduction. *Nature*. 402:47–52.

33. Ehrenreich, A., and F. Widdel. 1994. Anaerobic oxidation of ferrous iron by purple bacteria, a new type of phototrophic metabolism. *Appl. Environ. Microbiol.* 60:4517–4526.

34. Taboy, C. H., K. V. Vaughan, T. A. Mietzner, P. Aisen, and A. L. Crumbliss. 2001. Fe^{3+} coordination and redox properties of a bacterial transferrin. *J. Biol. Chem.* 276:2719–2724.

35. Gasdaska, J. R., J. H. Law, C. J. Bender, and P. J. Aisen. 1996. Cockroach transferrin closely resembles vertebrate transferrins in its metal ion-binding properties: a spectroscopic study. *J. Inorg. Biochem.* 64:247–258.

36. Dasgupta, J., R. T. van Willigen, and C. G. Dismukes. 2004. Consequences of structural and biophysical studies for the molecular mechanism of photosynthetic oxygen evolution: functional roles of calcium and bicarbonate. *Phys. Chem. Chem. Phys.* 6:4793–4802.

37. Ferreira, K. N., T. M. Iverson, K. Maghlaoui, J. Barber, and S. Iwata. 2004. Architecture of the photosynthetic oxygen evolving center. *Science*. 303:1831–1838.

38. Kurokawa, H., B. Mikami, and M. J. Hirose. 1995. Crystal structure of diferric hen ovotransferrin at 2.4 Å resolution. *J. Mol. Biol.* 254:196–207.

39. Sarra, R., R. Garratt, B. Gorinsky, H. Jhoti, and P. Lindley. 1990. High-resolution x-ray studies on rabbit serum transferrin: preliminary structure analysis of the N-terminal half-molecule at 2.3 Angstroms resolution. *Acta Crystallogr. B*. 46:763–771.

40. Cheng, Y., O. Zak, P. Aisen, S. C. Harrison, and T. Walz. 1994. Structure of the human transferrin receptor-transferrin complex. *Cell*. 116:565–576.